


Diffusion-induced stresses due to an impulsive mass source under non-Fickian mass transfer models

M. Fayik¹ , A.R. El-Dhaba² , E. Awad¹ 

¹Department of Mathematics, Faculty of Education, Alexandria University, Souter St. El-Shatby, Alexandria
P.O. box 21526, Egypt

²Department of Mathematics, Faculty of Science, Damanhur University, Egypt
 m_fayik@alexu.edu.eg

Abstract. The description of the mass transfer mechanisms in various physical and engineering fields, e.g., Li-ion batteries, is of significant importance for optimizing their performance. The present work introduces a comparative study describing the different responses of a perfectly elastic material when different non-Fickian diffusion situations are considered. The uncoupled theory of elastic diffusion, in which the diffusion process is described by non-Fickian laws, such as Cattaneo, Jeffreys-type, and Burgers-type constitutive laws, is employed in this modeling. The diffusion of lithium ions inside the silicon anode is one of the physical situations in which diffusion-induced stresses may be significant. An impulsive initial value problem, consisting of an initial lithium ions amount that starts impulsively to diffuse over the entire space of a silicon material, is considered. Direct approach together with Laplace and exponential Fourier transforms techniques are employed to obtain the solution in the Laplace transformed domain. The inverse Laplace transform is computed numerically to obtain the solution in the physical domain. Comparisons among the material responses to different diffusion regimes are presented.

Keywords: Cattaneo equation, Jeffreys equation, linear elasticity, lithium-ion batteries, impulsive problem

Acknowledgements. No external funding was received for this study. E.A. is grateful to Renat Sibatov for providing his work in Ref. [44] and for fruitful discussion.

Citation: Fayik M, El Dhaba AR, Awad E. Diffusion-induced stresses due to an impulsive mass source under non-Fickian mass transfer models. *Materials Physics and Mechanics*. 2023;51(1): 93-107. DOI: 10.18149/MPM.5112023_9.

Introduction

In the middle of the last century, Nabarro [1] suggested that the self-diffusion within the grains of a polycrystalline solid can cause the solid to "Yield", resulting in a change in the shape of the solid crystal. Herring [2] developed an underlying theory, based on Nabarro's suggestion, and presented the calculations of the rate of creeping. Generally speaking, the diffusion of solute atoms or molecules in solid materials, for example, gases in metal and lithium ions in the battery, creates diffusion-induced stress (or chemical stress) [3,4] and may cause fracture or dislocation of the local structure of the solvent [5]. Prussin [3] was the first author who referred to some estimates of the phenomenon of diffusion-induced stress. As for the diffusion and chemical stress interactions, Li [4] studied the stress-induced diffusion model in elastic materials. Yang [6] presented a diffusion equation based on the

effect of stress-induced diffusion and established a relationship between hydrostatic stress and the concentration of solute atoms, see also [7-10]. All these works altered the original structure of Fick's first law by replacing the concentration with the chemical potential. In this setting, they expressed the non-Fickian diffusion induced by the lattice distortions, in other words, the coupling between lattice stresses and diffusion. Although the fundamental hypothesis, in some works, is the coupling between stresses and diffusion, i.e., stress-induced diffusion and diffusion-induced stress, it seems that neglecting the inertial term in the conservation of momentum leads eventually to uncoupling elastic diffusion (diffusion-induced stress), see e.g., [11].

One of the early investigations that had shed light on the stress distributions resulting from possible non-Fickian mass diffusion mechanisms is the work of Povstenko [12], where the author expressed this anomaly by applying a fractional diffusion-wave equation and examined the effect of this non-Fickian diffusion on the stresses with disregarding the reverse effect of solvent's strain gradient on the diffusing particle flux (i.e. chemical potential is itself the concentration), see also the monograph [13] for further perspectives and applications.

Normal diffusion processes described by the second Fick's law, owing the fame linear time-dependence law of the mean-squared displacement (MSD) of the diffusive substance $\langle x^2(t) \rangle \propto t$, is not dominant in all diffusion situations. Instead, fluorescence spectroscopy experiments [14] and computer simulations [15] showed a non-linear behavior for the MSD, such as ballistic behavior in the short time, or crossover from linear in the short time to non-linear in the intermediate time. We further refer the reader to the comprehensive review [16] on such non-linear behaviors. Therefore, the normal diffusion equation is no longer valid to simulate such anomalous behaviors. Furthermore, the lagged response idea [17] with its well-known fundamental concepts (flux-precedence and gradient-precedence), suggesting the non-simultaneous response between the flux and the distribution gradient that eliminates the paradox of instantaneous propagation [18], comprises many macroscopic/microscopic heat and mass transfer models, e.g., Cattaneo equation [18-22] and Jeffreys equation [23-26]. The first attempt to model non-anomalous diffusion situations using Jeffreys equation by building a connection between Jeffreys equation and the two-phase model of mass transfer [27,28] that corresponds to the two-step model of ultrafast heat transfer [29,30], has been due to [23,24]. Despite the criticism of Jeffreys equation [31] and the hyperbolic Dual-Phase-Lag (DPL) equation [32], which shows negative values for the temperature in high dimensions, which in turn prevents these equations from modeling concentration of the diffusing substances, the authors [25,26] have derived the sufficient conditions for the probabilistic interpretation of Jeffreys equation and built a connection with the continuous-time random walk scheme. In spite of the defect of the hyperbolic DPL law, yielding negative values in higher dimensions, we can adopt it and its modified version [33] (or Burgers-like equation [34]) if the problem is one-dimensional. The reader can consult Quintanilla and Racke's conditions on the DPL equations for satisfying stability and well-posedness [35,36]. For other anomalous diffusion models in higher dimensions, we refer to recent studies [37,38].

The diffusion of lithium ions in a solid-state electrolyte is an engineering environment rich with anomalous situations which are in any way do not obey the linear behavior $\langle x^2(t) \rangle \propto t$, see e.g., [39-44]. In [39], the authors studied the segmental motion of $\text{CH}_2\text{CH}_2\text{O}/\text{CH}_2\text{CH}(\text{CH}_3)\text{O}$ moiety of the bulk solid-polymer electrolyte and the hopping motion of lithium ions (^7Li) activated by this segmental motion. They reported experimentally that the anions (negative ions) diffusion exhibits an anomalous behavior following $\langle x^2(t) \rangle \propto t^\gamma$ with $0 < \gamma < 1$. This anomalous behavior diminishes with the increase in temperature. Using a molecular dynamic approach, the study [42] reported different diffusion properties of lithium ions on different structure orientations of pure silicon. They emphasized the experimental results of [40, 41] that the diffusion is faster in $\langle 110 \rangle$ orientation compared with

other orientations $\langle 100 \rangle$ and $\langle 111 \rangle$ and requires a smaller critical force. Moreover, during the charging process of the battery, the pure silicon anode maintains its crystalline structure for a short period, thereafter it would be transformed into Li-Si alloy. Thus, the diffusion of lithium becomes an alloy with different lithium concentrations. The low-lithium concentrations alloy was found to act as a "cage-like" for the diffusing lithium ions. When the lithium concentration increased, the pure silicon would be entirely converted to Li-Si alloy structure, hence the caging effect of the silicon structure disappeared. From a theoretical viewpoint, studying the disorder-extent of the silicon structure due to discharging/charging (lithiation/delithiation) processes, requires "resetting" the velocity of diffusing lithium to zero after a certain time for avoiding the velocity from going to infinity. One of the other anomalous behaviors observed in lithium-ion batteries is the low-frequency impedance response of LiCoO₂/C batteries which makes with the real axis (in Z_{im}/Z_{re} Nyquist plot) an angle greater than 45° (the default angle for diffusion impedance known as the Warburg impedance). In [43], a mathematical description for the electrochemical impedance [45] based on a fractional kinetic approach was adopted for developing a model that describes the impedance response of LiCoO₂/C batteries by taking into account activation of the anomalous diffusion, see also [44,46] for other perspectives of anomalous diffusion in lithium-ion batteries and solids. To perfectly capture the inertia of lithium ions transport in graphitic materials, Maiza and coworkers [47] replaced the classical Fickian approach with the non-instantaneous response assumption represented by the single-phase-lag in the particle flux, in other words, the first approximation is Cattaneo equation or Maxwell-Cattaneo-Vernotte (MCV) equation. They compared the two approaches and found that the MCV approach, or alternatively, the lagging response in the particle flux, allows providing an interpretation of observed electrochemical behaviors.

The objective of the current study is to introduce a qualitative assessment of the response of solid solvent when four main types of non-Fickian diffusion events occur: Cattaneo equation; Jeffreys equation; hyperbolic DPL equation and modified hyperbolic DPL (Burgers-like) equation. It is concluded from this study to facilitate prior knowledge to simply recognize the response of the material to possible diffusion processes. We organize the paper as follows: In the next section, we formulate and solve an initial-value problem in elastic diffusion based on the different diffusion models. The first fundamental solution is brought in the Laplace domain. Numerical schemes, graphical representations, and potential discussions are prepared in Section 0. We give a summary of the work, concluding remarks, and future generalizations in Section 0.

Diffusion-induced stresses in an infinite domain

The diffusion of atoms or their ions (cations/anions) within a solvent medium causes distortions in the solvent lattice which could result in the development of local stresses that are known in the literature as diffusion-induced (or chemical) stresses [6-8]. Conversely, when the effect of stresses on the diffusion process is considered, then we have a stress-induced diffusion and Fick's first law is replaced with [2,48]

$$\mathbf{J}(\mathbf{r}, t) = -\frac{D_0}{R\theta} c(\mathbf{r}, t) \nabla \mu(\mathbf{r}, t), \quad (1)$$

where $\mathbf{J}(\mathbf{r}, t)$ is the particle flux vector, $\mathbf{r} \in \mathbb{R}^n$ denotes the position vector in the n th dimensional space, $\mathbf{r} = \langle x_1, \dots, x_n \rangle$, and t denotes the temporal variable, R is the gas constant, θ is the absolute temperature, D_0 is the diffusion coefficient and $\mu(\mathbf{r}, t)$ is the chemical potential determined through the constitutive relation [4]

$$\mu(\mathbf{r}, t) = R\theta \ln c(\mathbf{r}, t) - \Omega \sigma_H(\mathbf{r}, t) \quad (2)$$

where Ω is the partial molar volume (m³/mol) and $\sigma_H(\mathbf{r}, t)$ is the hydrostatic stress defined as the mean of normal stresses, namely,

$$\sigma_H = \frac{\sigma_{xx} + \sigma_{yy} + \sigma_{zz}}{3}. \quad (3)$$

In isothermal thermodynamical processes, the generalized Fick's law (1) with the chemical potential (2) reads

$$\mathbf{J}(\mathbf{r}, t) = -D_0 \left[\nabla c(\mathbf{r}, t) - \frac{\Omega}{R\theta} c(\mathbf{r}, t) \nabla \sigma_H(\mathbf{r}, t) \right]. \quad (4)$$

If the effect of stresses on the diffusion is negligible, or in other words, if we disregard the nonlinear terms of (4), we recover the classical Fick's first law $\mathbf{J}(\mathbf{r}, t) = -D_0 \nabla c(\mathbf{r}, t)$.

Because the main goal of this study is to introduce a comparative analysis that distinguishes the response of the solvent lattice to different types of non-Fickian diffusion, we assume that the lattice distortions (deformations) are very small and recoverable so that we can adopt the classical model of linear elasticity which describes the chemical stresses through the strain-stress constitutive relation [6]

$$\varepsilon_{ij} = \frac{1}{E} [(1 + \nu)\sigma_{ij} - \nu\sigma_{kk}\delta_{ij}] + \frac{\Omega}{3} c\delta_{ij}, \quad (5)$$

where σ_{ij} are the components of the stress tensor, ε_{ij} are the component of the strain tensor, $i, j = 1, 2, 3$, $\sigma_{kk} = \sigma_{xx} + \sigma_{yy} + \sigma_{zz}$ is the volumetric stress, δ_{ij} is the Kronecker delta, E and ν are Young's modulus and Poisson ratio of the elastic material. Setting $i = j$ in (5), we get the relation

$$\frac{E}{3(1 - 2\nu)} \varepsilon = \sigma_H + \frac{\Omega E}{3(1 - 2\nu)} c, \quad (6)$$

where $\sigma_{kk} = 3\sigma_H$, $\varepsilon = \varepsilon_{kk} = \varepsilon_{xx} + \varepsilon_{yy} + \varepsilon_{zz}$ is the volumetric strain, and the strain components are related to the displacement through the constitutive equation

$$\varepsilon_{ij} = \frac{1}{2} (u_{i,j} + u_{j,i}), \quad (7)$$

and $u = \langle u_x, u_y, u_z \rangle$ is the displacement vector. Now substituting from (6) into (5), we obtain the stress-strain constitutive relation

$$\sigma_{ij} = \frac{E}{1 + \nu} \varepsilon_{ij} + \frac{\nu E}{(1 + \nu)(1 - 2\nu)} \varepsilon \delta_{ij} - \frac{\Omega E}{3(1 - 2\nu)} c \delta_{ij}. \quad (8)$$

Here, we consider only the diffusion-induced stress with disregarding the stress-induced diffusion. Furthermore, we assume that different non-Fickian diffusion situations could occur during the simulation, so we have altered the classical Fick's first law $\mathbf{J}(\mathbf{r}, t) = -D_0 \nabla c(\mathbf{r}, t)$ with the following the more inclusive constitutive law [17,26]:

$$\mathbf{J}(\mathbf{r}, t + \tau_j) = -D_0 \nabla c(\mathbf{r}, t + \tau_c), \quad (9)$$

where τ_j and τ_c are constants of time dimension termed phase-lag in the diffusion flux and phase-lag in the concentration-gradient respectively. Equation (9) generalizes the approach followed in [47], wherein the phase lag τ_c has been neglected from their study. The first approximation of the Taylor series expansion of (9) yields the Jeffreys-type constitutive law

$$(1 + \tau_j \partial_t) \mathbf{J}(\mathbf{r}, t) = -D_0 (1 + \tau_c \partial_t) \nabla c(\mathbf{r}, t), \quad (10)$$

which leads to a parabolic type of partial differential equation. Whilst the second approximation of the Taylor series of the left-hand side of (9) yields the constitutive law

$$\left(1 + \tau_j \partial_t + \frac{\tau_j^2}{2} \partial_t^2 \right) \mathbf{J}(\mathbf{r}, t) = -D_0 (1 + \tau_c \partial_t) \nabla c(\mathbf{r}, t), \quad (11)$$

which gives a hyperbolic type of partial differential equation known as the hyperbolic DPL equation. Lastly, the successive lagging response of Fick's law yields the Burger-type constitutive law [33]

$$(1 + \tau_j \partial_t + \tau_m^2 \partial_t^2) \mathbf{J}(\mathbf{r}, t) = -D_0 (1 + \tau_c \partial_t) \nabla c(\mathbf{r}, t), \quad (12)$$

where that $\tau_j = \tau_{j_1} + \tau_{j_2}$, $\tau_m = \sqrt{\tau_{j_1}\tau_{j_2}}$, τ_{j_1} and τ_{j_2} are successive phase lags in the diffusion flux. Introducing the controlling parameters n_0 and n_1 , the above equations, (10)-(12), can be combined in the following generic constitutive law:

$$\left(1 + \tau_j \partial_t + \left(n_0 \frac{\tau_j^2}{2} + n_1 \tau_m^2\right) \partial_t^2\right) \mathbf{J}(\mathbf{r}, t) = -D_0(1 + \tau_c \partial_t) \nabla c(\mathbf{r}, t). \quad (13)$$

The numbers n_0 and n_1 , used in the above equation, take their values from the set $\{0,1\}$, and they are inserted for invoking various diffusion models from the single unphysical equation (13), that show up in the following limiting cases:

- (i) Equation (13) reduces to the well-known Fick's first law, if and only if $n_0 = n_1 = 0$, and the time constants are identical or neglected, $\tau_j = \tau_c = 0$.
- (ii) Cattaneo equation can be obtained from (13) when setting $n_0 = n_1 = 0$ and $\tau_c = 0$.
- (iii) The parabolic flux-precedence (flux-driven) Jeffreys equation is produced, when $n_0 = n_1 = 0$, and $\tau_j < \tau_c$.
- (iv) The parabolic concentration gradient-precedence Jeffreys equation is obtained, when $n_0 = n_1 = 0$, and $\tau_j > \tau_c$.
- (v) For $n_0 = 1, n_1 = 0$, equation (13) reduces to the hyperbolic DPL diffusion model.
- (vi) Setting $n_0 = 0, n_1 = 1, \tau_j > \tau_c$, equation (13) reduces to the modified hyperbolic DPL diffusion model or alternatively the Burgers-type equation, such that $\tau_j = \tau_{j_1} + \tau_{j_2}$, $\tau_m = \sqrt{\tau_{j_1}\tau_{j_2}}$, where τ_{j_1} and τ_{j_2} are successive phase lags in the diffusion flux.

Therefore, any local stress will be stimulated by the diffusion process only.

The conservation of momentum for the alloy (solvent and solute atoms) is given in the absence of external agents by

$$\sigma_{ji,j} = \rho \ddot{u}_i,$$

where $\rho = \rho_0 + \rho_{\text{alloy}}(c)$ is the density and ρ_0 is the density of the solvent at constant temperature (assumed constant). Because of the linearity assumption in this section, we neglect the term $\rho_{\text{alloy}}(c)\ddot{u}_i$ and keep only the linear term $\rho_0\ddot{u}_i$. Therefore, the conservation of momentum reads

$$\sigma_{ji,j} = \rho_0 \ddot{u}_i. \quad (14)$$

Likewise, we ignore the dependence of E and ν on the solute concentration and take them as material constants at a constant temperature. Under these assumptions, the initial value problem can be modeled in the one-dimensional setting where the displacement vector and the concentration of the solute are given as

$$\mathbf{u} = \langle u(x, t), 0, 0 \rangle, \quad c(\mathbf{r}, t) = c(x, t). \quad (15)$$

Thus, the normal stresses are given by

$$\sigma_{xx} = \frac{(1 - \nu)E}{(1 + \nu)(1 - 2\nu)} \epsilon - \frac{\Omega E}{3(1 - 2\nu)} c, \quad (16)$$

$$\sigma_{yy} = \sigma_{zz} = \frac{\nu E}{(1 + \nu)(1 - 2\nu)} \epsilon - \frac{\Omega E}{3(1 - 2\nu)} c, \quad (17)$$

and the hydrostatic stress is given by

$$\sigma_H = \frac{E}{3(1 - 2\nu)} [\epsilon - \Omega c]. \quad (18)$$

The equation of conservation of momentum has a nonzero component in x -direction, namely $\partial^2 \sigma_{xx} / \partial x^2 = \rho_0 \partial^2 \epsilon / \partial t^2$, which upon combining it with the constitutive relation (16), we obtain

$$\frac{(1 - \nu)E}{(1 + \nu)(1 - 2\nu)} \frac{\partial^2 \epsilon}{\partial x^2} - \frac{\Omega E}{3(1 - 2\nu)} \frac{\partial^2 c}{\partial x^2} = \rho_0 \frac{\partial^2 \epsilon}{\partial t^2}, \quad (19)$$

and the concentration is given by:

$$\left(1 + \tau_j \partial_t + \left(n_0 \frac{\tau_j^2}{2} + n_1 \tau_m^2\right) \partial_t^2\right) \frac{\partial c}{\partial t} = D_0(1 + \tau_c \partial_t) \frac{\partial^2 c}{\partial x^2}, \quad (20)$$

resulted from eliminating the flux $\mathbf{J}(\mathbf{r}, t)$ between (13) and the continuity equation:

$$\nabla \cdot \mathbf{J}(\mathbf{r}, t) + \frac{\partial c(\mathbf{r}, t)}{\partial t} = 0, \quad (21)$$

and considering the one-dimensional setting (15). For our impulsive initial value problem, we attach the following initial conditions

$$\begin{aligned} c(x, 0) &= c_0 \delta\left(\frac{x}{\sqrt{D_0 \tau_j}}\right), \quad \left.\frac{\partial c(x, t)}{\partial t}\right|_{t=0} = \frac{\tau_c D_0 c_0}{\tau_j} \partial_x^2 \left[\delta\left(\frac{x}{\sqrt{D_0 \tau_j}}\right)\right], \quad \epsilon(x, 0) \\ &= \left.\frac{\partial \epsilon(x, t)}{\partial t}\right|_{t=0} = 0. \end{aligned} \quad (22)$$

By applying the following transformations

$$\begin{aligned} \frac{x}{\sqrt{D_0 \tau_j}} &\rightarrow x, \quad \frac{u}{\sqrt{D_0 \tau_j}} \rightarrow u, \quad \frac{t}{\tau_j} \rightarrow t, \quad \frac{\Omega(1 + \nu)}{3(1 - \nu)} c \rightarrow c, \\ \frac{(1 + \nu)(1 - 2\nu) \sigma_{ij}}{1 - \nu} &\rightarrow \sigma_{ij}, \end{aligned} \quad (23)$$

the governing equations can be cast in the dimensionless form:

$$\frac{\partial^2 \epsilon}{\partial x^2} - \frac{\partial^2 c}{\partial x^2} = \kappa_M \frac{\partial^2 \epsilon}{\partial t^2}, \quad (24)$$

$$\left(1 + \partial_t + \left(\frac{n_0}{2} + n_1 \chi_1^2\right) \partial_t^2\right) \frac{\partial c}{\partial t} = (1 + \chi_0 \partial_t) \frac{\partial^2 c}{\partial x^2}, \quad (25)$$

$$\sigma_{xx} = \epsilon - c, \quad (26)$$

$$\sigma_{yy} = \sigma_{zz} = \frac{\nu}{1 - \nu} \epsilon - c \quad (27)$$

and the hydrostatic stress

$$\sigma_H = \kappa_S \epsilon - c \quad (28)$$

subject to the dimensionless initial conditions [22, 26]

$$c(x, 0) = \delta(x), \quad \left.\frac{\partial c(x, t)}{\partial t}\right|_{t=0} = \chi_0 \partial_x^2 [\delta(x)], \quad \epsilon(x, 0) = \left.\frac{\partial \epsilon(x, t)}{\partial t}\right|_{t=0} = 0 \quad (29)$$

where

$$\kappa_M = \frac{\varrho_0 D_0 (1 + \nu)(1 - 2\nu)}{\tau_j (1 - \nu) E}, \quad \kappa_S = \frac{1 + \nu}{3(1 - \nu)}, \quad \chi_0 = \frac{\tau_c}{\tau_j}, \quad (30)$$

$$\chi_1 = \frac{\tau_m}{\tau_j}, \quad c_0 = \frac{3(1 - \nu)}{\Omega(1 + \nu)}.$$

The solutions of (24)-(25) subject to (29) are given in the Laplace-Fourier space as

$$\hat{\hat{\epsilon}}(q, s) = \frac{L(s)}{\kappa_M s^2 - sL(s)} \left[\frac{\kappa_M s^2}{q^2 + \kappa_M s^2} - \frac{sL(s)}{q^2 + sL(s)} \right], \quad (31)$$

$$\hat{\hat{c}}(q, s) = \frac{L(s)}{q^2 + sL(s)}, \quad (32)$$

where

$$\tilde{L}(s) = \frac{\left(1 + s + \left(\frac{n_0}{2} + n_1 \chi_1^2\right) s^2\right)}{1 + \chi_0 s}. \quad (33)$$

Here, the tildes refer to the Laplace transform $\tilde{f}(x, s) = \mathcal{L}\{f(x, t); t\}(x, s) = \int_0^\infty f(x, t) \exp(-st) dt$, the hats refer to the Fourier transform $\hat{f}(q, t) =$

$\mathcal{F}\{f(x, t); x\}(q, t) = \int_{-\infty}^{\infty} f(x, t) \exp(iqx) dx$, $s \in \mathbb{C}$ is the Laplace parameter, and $q \in \mathbb{R}$ is the Fourier parameter.

Finding a closed-form expression for the volumetric strain $\hat{\epsilon}(q, s)$ in the real domain is an intractable problem to our knowledge. To extract as much information as possible from the above simulation, we shall at first invert the Fourier transform using a well-known tabulated rule, then we invoke to a familiar numerical technique to invert the Laplace transform. The solutions of the volumetric strain and the concentration are given in the Laplace space:

$$\tilde{\epsilon}(x, s) = \frac{L(s)}{2(\kappa_M s^2 - sL(s))} \left[\sqrt{\kappa_M s^2} \exp\left(-\sqrt{\kappa_M s^2}|x|\right) - \sqrt{sL(s)} \exp\left(-\sqrt{sL(s)}|x|\right) \right] \quad (34)$$

$$\tilde{c}(x, s) = \frac{1}{2} \sqrt{\frac{L(s)}{s}} \exp\left(-\sqrt{sL(s)}|x|\right), \quad (35)$$

where we have used the rule $\mathcal{F}^{-1}\left\{\frac{1}{a^2 + \omega^2}\right\} = \frac{1}{2a} \exp(-a|x|)$, see [49].

Results and discussions

In this section we bring the solutions of concentration and volumetric strain to the real domain by inverting numerically the Laplace transform in equations (34)-(35), [17,50-55]. The diffusion of lithium ions in silicon anode is chosen for this simulation. Because of the phenomenological nature of our study, we have considered an infinite silicon medium and there has been an impulse of lithium ions distributed uniformly on the yz -plane ($x = 0$). No surprising that if the phenomenon occurs on the picometer scale, the micrometer silicon film can be considered as a half-space. The crystalline silicon parameters at room temperature $\theta_0 = 298K$ are [8] $E = 159 GPa$, $\nu = 0.22$, and the density [56] $\rho_0 = 2.33 \times 10^3 Kg/m^3$. The diffusivity of lithium ions in the silicon at room temperature $\theta_0 = 298K$ is $D_0 = 10^{-17} m^2/s$ [8] and the partial molar volume $\Omega = 7.69 \times 10^{-6} m^3/mol$. Further, we have chosen the relaxation of particle flux as $\tau_j = 10^{-15} = 1 \text{ femtosecond}$. Using these parameters, we have

$$\kappa_M = 0.128, \kappa_S = 0.521, c_0 = 2.494 \times 10^5, \quad (36)$$

and χ_0 and χ_1 will be arbitrarily chosen to study the effects of the concentration gradient and flux diffusion delay, respectively.

Figure 1 shows the hydrostatic stress at different values of time for the Fickian diffusion. In the short time domain, the propagation of discontinuities, a characteristic property in the mathematical model of linear elasticity [57] and coupled thermoelasticity [58], is clear. As time progresses, the discontinuities go to infinity so that they do not appear in the long-time domain near the disturbances as Fig. 1(b) shows. In the finite-speed diffusion governed by the telegrapher "Cattaneo" equation, there is a characteristic discontinuity in the concentration profile in the short-time domain when the particle has had time to interact with the reflecting point [20]. This feature affects the corresponding stress distribution as shown in Fig. 2, where there are four discontinuity points for the single hydrostatic stress profile; two of them are due to the mechanical wave and the others are due to the concentration wave. With the passage of time, the wave term effect in the Cattaneo equation diminishes and the process transforms to the Fickian diffusion, thereby the discontinuity points due to finite-speed diffusion diminish in the intermediate time domain as Fig. 2(b). The long-time behavior of the hydrostatic stress due to finite-speed diffusion coincides with the long-time behavior of the Fickian diffusion, Fig. 1(b). Not only the temporal progress that lowers the sharpness of discontinuity points, but also the transition from telegrapher to telegrapher-like behavior as Fig. 3 exhibits.

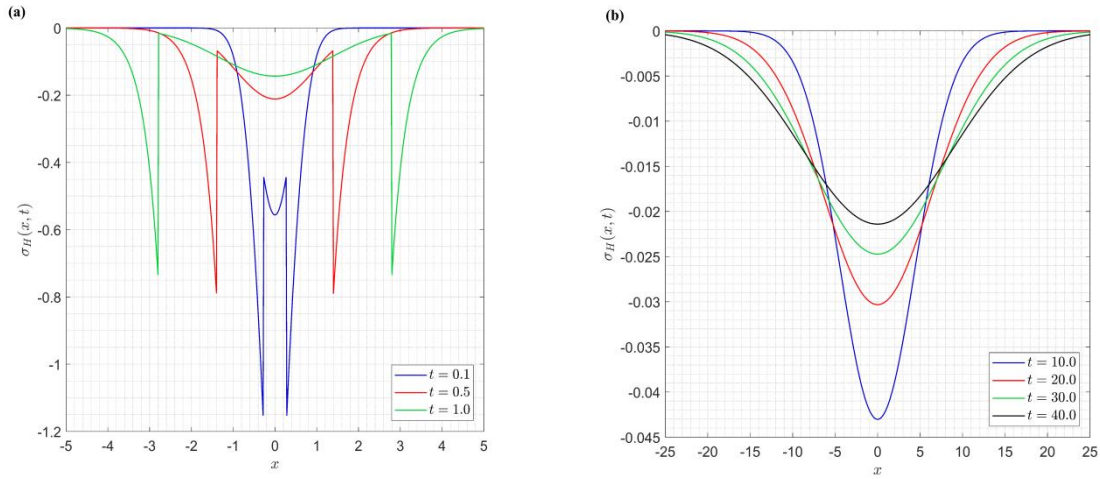


Fig. 1. Hydrostatic stress distribution for Fickian diffusion at different values of time: (a) for a small value of time; (b) for a large value of time

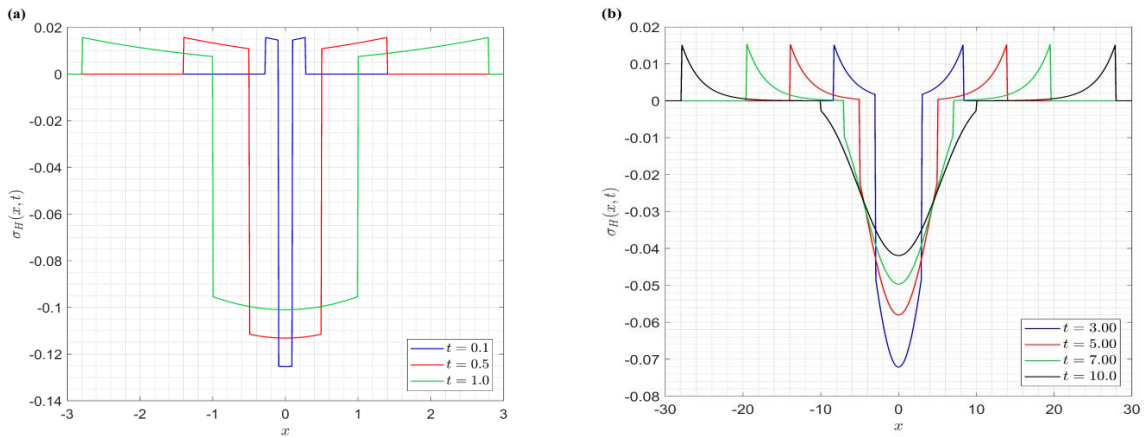


Fig. 2. Hydrostatic stress distribution for finite-velocity diffusion at different values of time: (a) for a small value of time; (b) for a large value of time

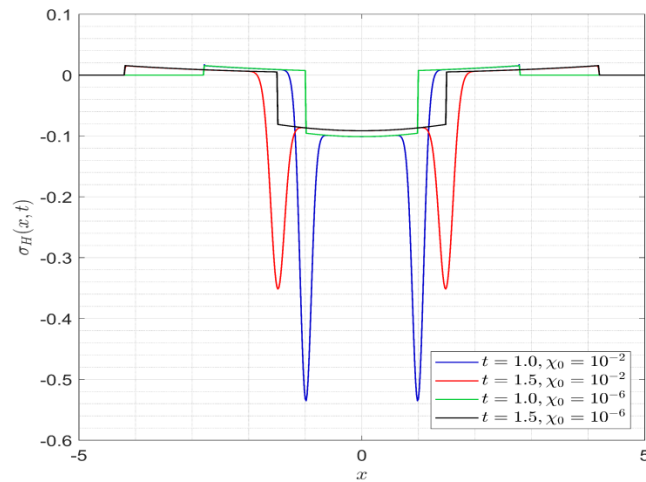


Fig. 3. Elimination of the discontinuity point of the finite-speed diffusion at the transition from telegrapher to telegrapher-like behavior

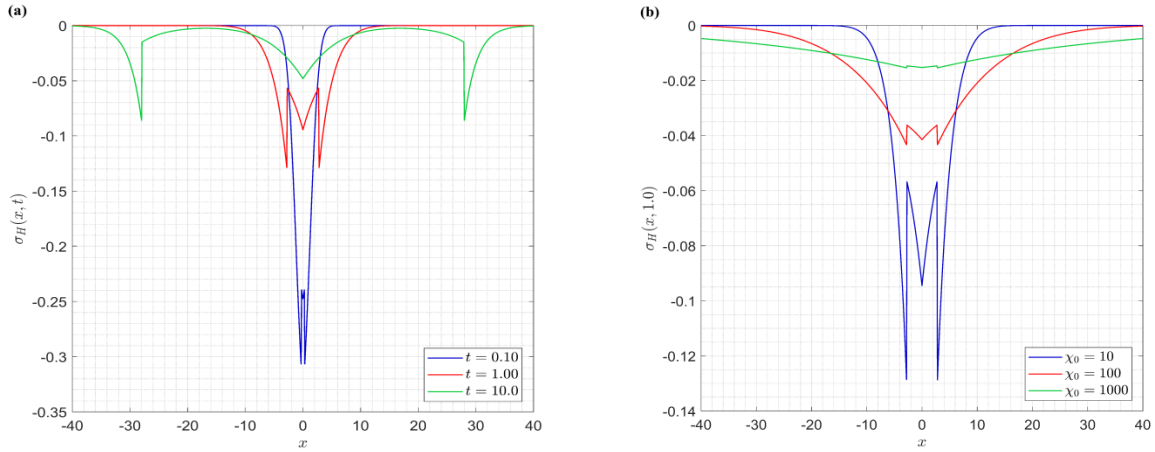


Fig. 4. Hydrostatic stress distribution for the DPL with flux precedence, or the cage-like diffusion: (a) for different values of time and $\chi_0 = 10$; (b) for different values of χ_0 and $t = 1.0$

As the ratio χ_0 leaves the interval $(0,1]$, i.e., $\tau_c > \tau_j$, the concentration profile described by ordinary Jeffreys equation converts from the telegrapher-like effect to the cage-like or the labyrinth-like effects characterized by the crossover from normal diffusion $\langle x^2(t) \rangle \propto t$ in the short-time domain to anomalous $\langle x^2(t) \rangle \propto t^\gamma$, $0 < \gamma < 1$ in the intermediate-time domain, and lastly from anomalous to normal again $\langle x^2(t) \rangle \propto t$ in the long-time domain, see [26]. The hydrostatic stress corresponding to this cage-like phenomenon at $\chi_0 = 10$ is depicted in Fig. 4(a) at relatively small values of the time. In comparison between the material response to the Fickian diffusion, Fig. 1(a), and to the diffusion with caging at random places within the solvent, Fig. 4(a), one concludes that the stresses in the diffusion process with caging have amplitudes less than those in the normal diffusion without caging or labyrinth, but the stresses in the case of caging reach to deeper points of the solvent compared to the normal diffusion situation. In view of Fig. 4(b) one can see that the longer the concentration gradient delays, the least-value and the deeper-distributed stresses within the solvent are.

In the ordinary wave equation, we have the dimensionless from

$$\frac{\partial^2 c}{\partial t^2} = \frac{\partial^2 c}{\partial x^2} \quad (37)$$

subject to

$$c(x, 0) = \delta(x), \quad \left. \frac{\partial c(x, t)}{\partial t} \right|_{t=0} = 0, \quad (38)$$

which can be obtained from Eq. (25) by setting $n_0 = 0, n_1 = 1$, and $\chi_0 = 0$. The first fundamental solution of the wave equation (37), i.e., the initial conditions (38) are considered, in the Laplace-Fourier domain reads $\hat{c}(q, s) = s/(s^2 + q^2)$, which can be solved analytically as [59]

$$c_{\text{wave}}(x, t) = \frac{1}{2} \delta(t - |x|). \quad (39)$$

The solution (39) is zero everywhere except at the points $x = \pm t$, where it goes to infinity at these points. Inserting this solution into Eq. (24) as an external agent stimulating the lattice strain, we get

$$\epsilon(x, t) = \frac{1}{2(1 - \kappa_M)} [\delta(t - |x|) - \sqrt{\kappa_M} \delta(t - \sqrt{\kappa_M} |x|)], \quad (40)$$

and substituting the resulting volumetric strain (40) and the concentration (39) into the hydrostatic stress (28) we obtain

$$\sigma_H(x, t) = \frac{1}{2(1 - \kappa_M)} [(\kappa_M + \kappa_S - 1)\delta(t - |x|) - \kappa_S \sqrt{\kappa_M} \delta(t - \sqrt{\kappa_M} |x|)]. \quad (41)$$

Therefore, the hydrostatic stress (41) resulting from the ballistic motion of the dispersed substance is zero everywhere except at the four points $x = \pm t, \pm \frac{t}{\sqrt{\kappa_M}}$, where the stresses go to infinity also, which refers to the possibility of damaging the solvent medium at these points. It is noteworthy to mention that if we replace the conditions (38) with

$$c(x, 0) = 0, \quad \left. \frac{\partial c(x, t)}{\partial t} \right|_{t=0} = \delta(x), \quad (42)$$

we get the second fundamental solution of the wave equation [12]

$$c_{\text{wave}}(x, t) = \frac{1}{2} H(t - |x|). \quad (43)$$

It is noted that the second fundamental solution (43) has not a probabilistic interpretation since $\int_{-\infty}^{\infty} c_{\text{wave}}(x, t) dx = \frac{1}{2} \int_{-\infty}^{\infty} H(t - |x|) dx = t (\neq 1)$. Thus, we could not classify the motion following the distribution (43) with a certain dynamical description as the case of the second Fick's law and Cattaneo, and Jeffreys equations. For the sake of completeness in this discussion, we insert the solution (43) into Eqs (24) and (28), and we obtain

$$\epsilon(x, t) = \frac{1}{2(1 - \kappa_M)} [H(t - |x|) - \sqrt{\kappa_M} H(t - \sqrt{\kappa_M}|x|)], \quad (44)$$

$$\sigma_H(x, t) = \frac{1}{2(1 - \kappa_M)} [(\kappa_M + \kappa_S - 1)H(t - |x|) - \kappa_S \sqrt{\kappa_M} H(t - \sqrt{\kappa_M}|x|)]. \quad (45)$$

The volumetric strain and the hydrostatic stress were not found in the first problem [12]. We present the hydrostatic stresses induced by the nonzero concentration-velocity at the beginning (45) in Fig. 5 at different values of the time. The four discontinuity points at $x = \pm t, \pm \frac{t}{\sqrt{\kappa_M}}$ are obvious. The two points $x = \pm t$ come from the wave motion, while the others $x = \pm \frac{t}{\sqrt{\kappa_M}}$ come from the mechanical wave, refer to Eqs. (43)-(45). We note the same velocities and discontinuity points in the hydrostatic stress resulting from the finite-speed diffusion in the short-time limit, refer to Fig. 2(a).

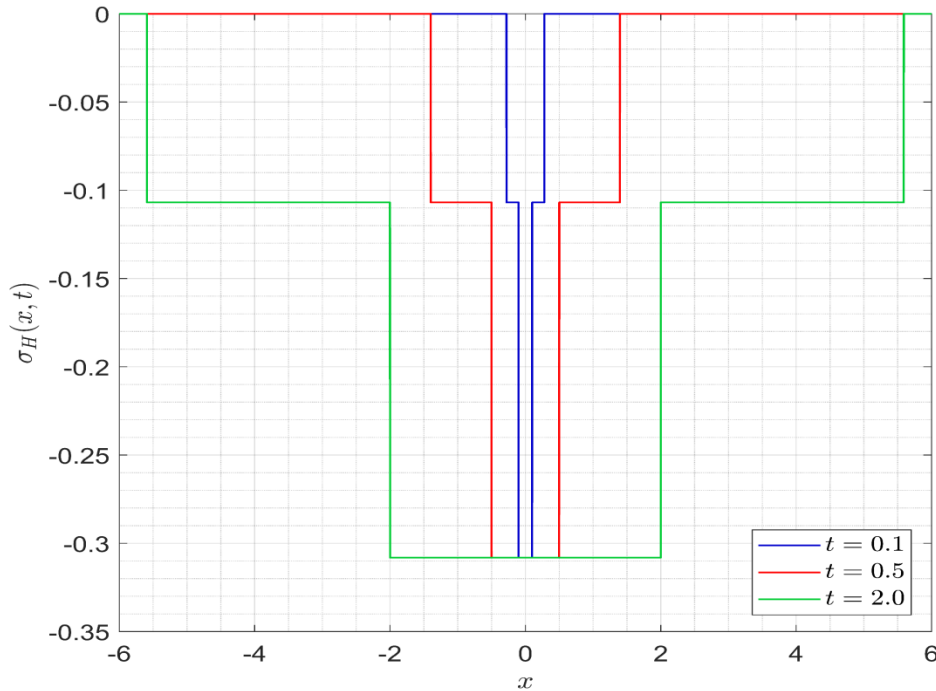


Fig. 5. Hydrostatic stress induced by an initial nonzero concentration velocity at different values of time

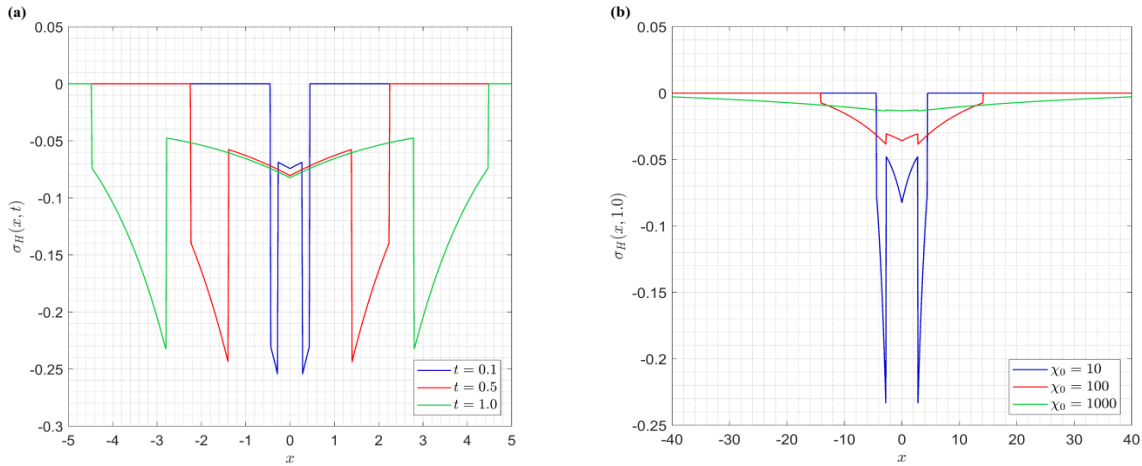


Fig. 6. Hydrostatic stress distribution for hyperbolic DPL diffusion model: (a) for different values of time, where $\chi_0 = 10$, (b) for different values of χ_0 , where $t = 1.0$

Figure 6(a) illustrates the distributions of hydrostatic stress governed by the hyperbolic DPL diffusion model at $\chi_0 = 10$, for short times. It is found that for any fixed short time, the mechanical, and diffusive waves are travelling with finite speeds, namely $\left(\frac{1}{\sqrt{\kappa_M}}, \sqrt{2\chi_0}\right)$, respectively. i.e., the hydrostatic stress has four discontinuity points at the locations $x = \pm\sqrt{2\chi_0}t, \pm\frac{t}{\sqrt{\kappa_M}}$. Also, for the fixed value of χ_0 , we note that the magnitude of mechanical wavefronts is the same at different values of time (independent of time or position), but the magnitude of diffusive wavefronts decreases as time passes (exponentially decreasing with x). Figure 6(b) shows the distributions of hydrostatic stress governed by the hyperbolic DPL diffusion model for different values of $\chi_0 > 1$, at instant $t = 1.0$. We can observe that as χ_0 increases, the hydrostatic stress records lower peaks, while the diffusive wave goes further into the medium because its speed increases, $v_{DPL} = \sqrt{2\chi_0}$. As far as there is a significant delay between the concentration gradient and the particle flux such that $\tau_c \gg \tau_j$ or $\chi_0 \gg 1$, then the diffusive wave speed becomes greater than the mechanical wave speed, i.e., $v_{DPL} \gg v_{Mech}$, which makes the diffusion process is dominant, particularly in the short-time domain. This statement is valid only for the diffusion of lithium ions in silicon medium since the coefficient κ_M will be different for other diffusion circumstances, and thus the mechanical wave speed will differ, $v_{Mech} = 1/\sqrt{\kappa_M}$. On the contrary, the case of Cattaneo diffusion equation is characterized by the relation $v_{Cattaneo} < v_{Mech}$, where $v_{Cattaneo} = 1$ and $v_{Mech} = 1/\sqrt{\kappa_M}$, which leads to the dominance of mechanical waves in the short-time domain.

Figure 7(a) illustrates the distributions of hydrostatic stress associated with the modified hyperbolic DPL diffusion model at $\chi_0 = 10$ and $\chi_1 = 0.246$ as time elapses. In this case, the mechanical and the diffusive waves are travelling with finite speeds $\left(\frac{1}{\sqrt{\kappa_M}}, \frac{\sqrt{\chi_0}}{\chi_1}\right)$, respectively, with finite sharp jumps at the wavefronts $x = \pm\frac{\sqrt{\chi_0}}{\chi_1}t, \pm\frac{t}{\sqrt{\kappa_M}}$, as shown in Fig. 7(a) at $t = 0.1, 0.5$ and 1 . Figure 7(b) clearly reveals that at any instant, for example at $t = 1.0$, the increasing of χ_1 at a fixed value of χ_0 leads to the magnitude of hydrostatics stress governed by modified hyperbolic DPL records the small values through interval domain $|x| < \frac{t}{\sqrt{\kappa_M}}$, and after crossing the mechanical wavefront, the increasing of $0 < \chi_1 < 1$ has a converse effect

on the domain $\frac{t}{\sqrt{\kappa_M}} < |x| < \frac{\sqrt{\chi_0}}{\chi_1} t$. In addition, the magnitude of the mechanical and diffusive wavefronts increases as χ_1 increases.

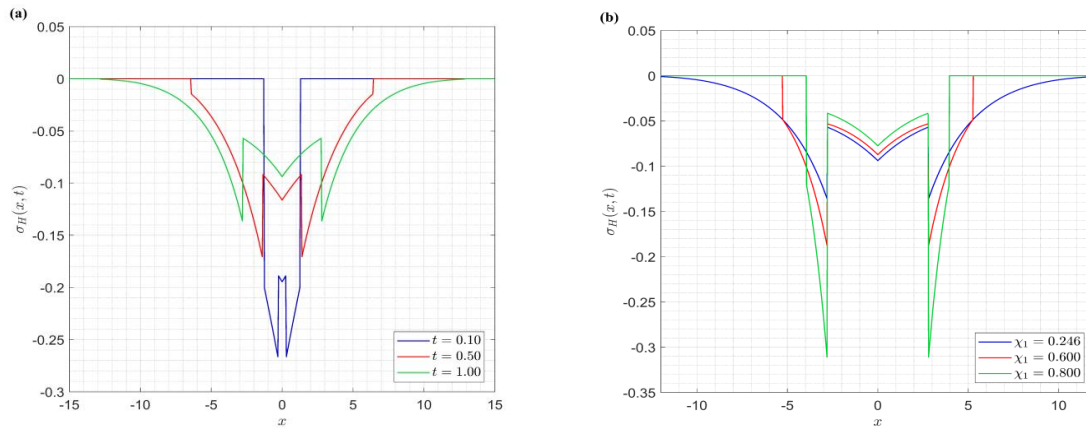


Fig. 7. Hydrostatic stress distribution for modified hyperbolic DPL diffusion model: (a) for different values of time, $\chi_0 = 10.0$ and $\chi_1 = 0.246$; (b) for different values of χ_1 , $\chi_0 = 10$ and $t = 1.0$

We infer that the hydrostatic stress governed by the Fickian diffusion, DPL with flux-precedence $\chi_0 \gg 1$, hyperbolic DPL, and modified hyperbolic DPL are compressive along the whole domain. The maximum value of the compressive stress is at the location of the mechanical wavefronts. Otherwise, the hydrostatic stress is governed by the Cattaneo and the Cattaneo-like diffusion (the gradient-precedence case in which $\chi_0 \ll 1$) equations is negative on the region $|x| < t$ (compressive stress region). After crossing the point $|x| = t$, the hydrostatic stress values transform suddenly to be positive, i.e., tensile stress region. In addition, the maximum values of compressive and tensile stresses are at the location of the mechanical and diffusive wavefronts. In this case, fracture failure is most likely to occur [60].

Conclusions

On a phenomenological basis, we introduced the generalized DPL equation to the uncoupled theory of elastic diffusion to compare the different responses of the material to these varieties of non-Fickian diffusion processes. We paid great attention to the hydrostatic stresses (chemical) inherent within the material. We found that the stresses record higher values in the normal and Fickian diffusion processes compared with the considered non-Fickian situations. Many investigations employed Fick's law for modeling the diffusion of solute atoms within a solid, e.g., the diffusion of lithium ions within the silicon. The stresses resulting from such investigations contain both the effect of diffusion on stress and the effect of stress on diffusion. We derived our motivation from the fundamental hypothesis of a recent investigation that studied the effect of delayed constitutive law on the diffusion of lithium ions, see [47], without discussing the stresses. Here, we discussed the stresses due to finite-speed diffusion, refer to Fig. 2, in addition to investigating the effect of other non-Fickian diffusion models on diffusion-induced stresses. We compared among the different velocities of the hyperbolic diffusion models and the mechanical wave velocities. The speed of diffusive waves governed by Cattaneo equation has apparently a velocity less than the mechanical wave speed in the case of diffusion of lithium ions within the silicon medium. Then, the mechanical waves dominate the short-time domain. On the contrary, the hyperbolic DPL diffusion models own speeds greater than the mechanical wave speed, thus, the diffusion process dominates the short-time domain.

References

1. Nabarro F. Report of a Conference on the Strength of Solids. In: *The Physical Society*. London; 1948. p.590.
2. Herring C. Diffusional viscosity of a polycrystalline solid. *J. Appl. Phys.* 1950;21(5): 437-45.
3. Prussin S. Generation and distribution of dislocations by solute diffusion. *J. Appl. Phys.* 1961;32(10): 1876-1881.
4. Chen-Min Li J. *Physical chemistry of some microstructural phenomena*. Springer; 1978.
5. Abbaschian R, Reed-Hill RE. *Physical Metallurgy Principles-SI Version: Cengage Learning*. 2009.
6. Yang F. Interaction between diffusion and chemical stresses. *Materials Science and Engineering: A*. 2005;409(1-2): 153-159.
7. Yang F. Effect of local solid reaction on diffusion-induced stress. *J. Appl. Phys.* 2010;107(10): 103516.
8. Yang F. Insertion-induced expansion of a thin film on a rigid substrate. *Journal of Power Sources*. 2013;241: 146-149.
9. Suo Y, Yang F. Transient analysis of diffusion-induced stress: effect of solid reaction. *Acta Mechanica*. 2019;230(3): 993-1002.
10. Chiang D, Ouyang H, Yang F, Lee S. An alternative method of solvent-induced stresses in an elastic thin slab: Moutier theorem. *Polymer Engineering & Science*. 2022;62(4): 1178-1186.
11. Wang X, Liu X, Yang Q. Transient analysis of diffusion-induced stress for hollow cylindrical electrode considering the end bending effect. *Acta Mechanica*. 2021;232(9): 3591-3609.
12. Povstenko Y. Stresses exerted by a source of diffusion in a case of a non-parabolic diffusion equation. *International Journal of Engineering Science*. 2005;43(11-12): 977-991.
13. Povstenko Y. *Fractional Thermoelasticity*. Springer; 2015.
14. Kubečka J, Uhlík F, Košovan P. Mean squared displacement from fluorescence correlation spectroscopy. *Soft Matter*. 2016;12(16): 3760-3769.
15. Bolintineanu DS, Grest GS, Lechman JB, Silbert LE. Diffusion in jammed particle packs. *Phys Rev Lett*. 2015;115(8): 088002.
16. Metzler R, Klafter J. The random walk's guide to anomalous diffusion: A fractional dynamics approach. *Physics Reports*. 2000;339(1): 1-77.
17. Tzou DY. *Macro-to microscale heat transfer: The lagging behavior*. 2nd ed. John Wiley & Sons; 2014.
18. Cattaneo C. A form of heat conduction equation which eliminates the paradox of instantaneous propagation. *Compte Rendus*. 1958;247(4): 431-433.
19. Compte A, Metzler R. The generalized Cattaneo equation for the description of anomalous transport processes. *Journal of Physics A: Mathematical and General*. 1997;30(21): 7277.
20. Masoliver J, Weiss GH. Finite-velocity diffusion. *European Journal of Physics*. 1996;17(4): 190.
21. Awad E. On the time-fractional Cattaneo equation of distributed order. *Physica A: Statistical Mechanics and its Applications*. 2019;518: 210-233.
22. Awad E, Metzler R. Crossover dynamics from superdiffusion to subdiffusion: Models and solutions. *Fractional Calculus and Applied Analysis*. 2020;23(1): 55-102.
23. Rukolaine SA, Samsonov AM. (Eds.) A model of diffusion, based on the equation of the Jeffreys type. In: *Proceedings of the International Conference Days on Diffraction 2013*. IEEE; 2013.

24. Rukolaine SA, Samsonov AM. Local immobilization of particles in mass transfer described by a Jeffreys-type equation. *Physical Review E*. 2013;88(6): 062116.
25. Awad E. Dual-Phase-Lag in the balance: Sufficiency bounds for the class of Jeffreys' equations to furnish physical solutions. *Int. J. Heat Mass Trans.* 2020;158: 119742.
26. Awad E, Sandev T, Metzler R, Chechkin A. From continuous-time random walks to the fractional Jeffreys equation: Solution and applications. *Int. J. Heat Mass Transf.* 2021;181C: 121839.
27. Sprague BL, Pego RL, Stavreva DA, McNally JG. Analysis of binding reactions by fluorescence recovery after photobleaching. *Biophysical Journal*. 2004;86(6): 3473-3495.
28. Beaudouin J, Mora-Bermúdez F, Klee T, Daigle N, Ellenberg J. Dissecting the contribution of diffusion and interactions to the mobility of nuclear proteins. *Biophysical Journal*. 2006;90(6): 1878-1894.
29. Anisimov SI, Kapeliovich BL, Perel'man TL. Electron emission from metal surfaces exposed to ultra-short laser pulses. *Sov Phys JETP*. 1974;39(2): 375-377.
30. Qiu TQ, Tien CL. Short-pulse laser heating on metals. *International Journal of Heat and Mass Transfer*. 1992;35(3): 719-726.
31. Rukolaine SA. Unphysical effects of the dual-phase-lag model of heat conduction. *International Journal of Heat Mass Transfer*. 2014;78: 58-63.
32. Rukolaine SA. Unphysical effects of the dual-phase-lag model of heat conduction: higher-order approximations. *International Journal of Thermal Sciences*. 2017;113: 83-88.
33. Awad E. On the generalized thermal lagging behavior: Refined aspects. *Journal of Thermal Stresses*. 2012;35(4): 293-325.
34. Quintanilla R, Rajagopal KR. On burgers fluids. *Mathematical Methods in the Applied Sciences*. 2006;29(18): 2133-2147.
35. Quintanilla R, Racke R. A note on stability in dual-phase-lag heat conduction. *International Journal of Heat and Mass Transfer*. 2006;49(7-8): 1209-1213.
36. Quintanilla R, Racke R. Qualitative aspects in dual-phase-lag heat conduction. *Proceedings of the Royal Society A: Mathematical, Physical and Engineering Sciences*. 2007;463(2079): 659-674.
37. Awad E, Sandev T, Metzler R, Chechkin A. Closed-form multi-dimensional solutions and asymptotic behaviors for subdiffusive processes with crossovers: I. Retarding case. *Chaos, Solitons & Fractals*. 2021;152C: 111357.
38. Awad E, Metzler R. Closed-form multi-dimensional solutions and asymptotic behaviours for subdiffusive processes with crossovers: II. Accelerating case. *Journal of Physics A: Mathematical and General*. 2022;55(20): 205003.
39. Hayamizu K, Aihara Y, Price WS. Correlating the NMR self-diffusion and relaxation measurements with ionic conductivity in polymer electrolytes composed of cross-linked poly (ethylene oxide-propylene oxide) doped with $\text{LiN}(\text{SO}_2\text{CF}_3)_2$. *The Journal of Chemical Physics*. 2000;113(11): 4785-4793.
40. Lee SW, McDowell MT, Choi JW, Cui Y. Anomalous shape changes of silicon nanopillars by electrochemical lithiation. *Nano Letters*. 2011;11(7): 3034-3039.
41. Pharr M, Zhao K, Wang X, Suo Z, Vlassak JJ. Kinetics of initial lithiation of crystalline silicon electrodes of lithium-ion batteries. *Nano Letters*. 2012;12(9): 5039-5047.
42. Wang H, Ji X, Chen C, Xu K, Miao L. Lithium diffusion in silicon and induced structure disorder: A molecular dynamics study. *AIP Advances*. 2013;3(11): 112102.
43. Erol S, Orazem ME. The influence of anomalous diffusion on the impedance response of LiCoO_2/C batteries. *Journal of Power Sources*. 2015;293: 57-64.
44. Sibatov RT, Svetukhin VV, Kitsyuk EP, Pavlov AA. Fractional differential generalization of the single particle model of a lithium-ion cell. *Electronics*. 2019;8(6): 650.

45. Bisquert J, Compte A. Theory of the electrochemical impedance of anomalous diffusion. *Journal of Electroanalytical Chemistry*. 2001;499(1): 112-120.
46. Uchaikin VVe, Sibatov R. *Fractional kinetics in solids: anomalous charge transport in semiconductors, dielectrics, and nanosystems*. World Scientific; 2013.
47. Maiza M, Mammeri Y, Nguyen DA, Legrand N, Desprez P, Franco A. Evaluating the impact of transport inertia on the electrochemical response of lithium ion battery single particle models. *Journal of Power Sources*. 2019;423: 263-270.
48. Bardeen J. Diffusion in binary alloys. *Phys Rev*. 1949;76(9): 1403.
49. Erdelyi A, Magnus W, Oberhettinger F, Tricomi FG. *Tables of integral transforms: Based in part on notes left by Harry Bateman and compiled by the staff of the Bateman manuscript project*. New York: McGraw-Hill Book Company; 1954.
50. Sherief HH, Dhaliwal RS. Generalized one-dimensional thermal-shock problem for small times. *Journal of Thermal Stresses*. 1981;4(3-4): 407-20.
51. Sherief HH, Hamza F, Abd El-Latif A. 2D problem for a half-space in the generalized theory of thermo-viscoelasticity. *Mechanics of Time-Dependent Materials*. 2015;19(4): 557-568.
52. Awad E, El Dhaba AR, Fayik M. A unified model for the dynamical flexoelectric effect in isotropic dielectric materials. *European Journal of Mechanics-A/Solids*. 2022;95: 104618.
53. Ezzat MA, Awad ES. Constitutive relations, uniqueness of solution, and thermal shock application in the linear theory of micropolar generalized thermoelasticity involving two temperatures. *Journal of Thermal Stresses*. 2010;33(3): 226-50.
54. Ezzat MA, Awad ES. Micropolar generalized magneto-thermoelasticity with modified Ohm's and Fourier's laws. *Journal of Mathematical Analysis and Applications*. 2009;353(1): 99-113.
55. Ezzat MA, El-Bary AA, Fayik MA. Fractional Fourier law with three-phase lag of thermoelasticity. *Mechanics of Advanced Materials and Structures*. 2013;20(8): 593-602.
56. Kalnaus S, Rhodes K, Daniel C. A study of lithium ion intercalation induced fracture of silicon particles used as anode material in Li-ion battery. *Journal of Power Sources*. 2011;196(19): 8116-24.
57. Boley BA. Discontinuities in integral-transform solutions. *Quarterly of Applied Mathematics*. 1962;19(4): 273-284.
58. Boley BA, Hetnarski RB. *Propagation of discontinuities in coupled thermoelastic problems*. 1968.
59. Schneider W, Wyss W. Fractional diffusion and wave equations. *Journal of Mathematical Physics*. 1989;30(1): 134-144.
60. Chu J, Lee S. Diffusion-induced stresses in two-phase elastic media. *International Journal of Engineering Science*. 1990;28(11): 1085-1109.

THE AUTHORS

Fayik M. 

e-mail: m_fayik@alexu.edu.eg

El-Dhaba A.R. 

e-mail: a.r.eldhaba@sci.dmu.edu.eg

Awad E. 

e-mail: emadawad78@alexu.edu.eg